The LINNEAN SOCIETY of London BIOLOGICAL Journal of the Linnean Society

*Biological Journal of the Linnean Society*, 2013, **108**, 586–599. With 6 figures

# Mandible allometry in extant and fossil Balaenopteridae (Cetacea: Mammalia): the largest vertebrate skeletal element and its role in rorqual lunge feeding

NICHOLAS D. PYENSON[1,2]*, JEREMY A. GOLDBOGEN[3] and ROBERT E. SHADWICK[4]

[1]*Department of Paleobiology, National Museum of Natural History, Smithsonian Institution, P.O. Box 37012, Washington, DC, 20013-7013, USA*
[2]*Departments of Mammalogy and Paleontology, Burke Museum of Natural History and Culture, Seattle, WA 98195, USA*
[3]*Cascadia Research Collective, 218½ West 4th Avenue, Olympia, WA, USA*
[4]*Department of Zoology, University of British Columbia, 6270 University Boulevard, Vancouver, BC, Canada V6T 1Z4*

*Received 4 July 2012; revised 10 September 2012; accepted for publication 10 September 2012*

Rorqual whales (crown Balaenopteridae) are unique among aquatic vertebrates in their ability to lunge feed. During a single lunge, rorquals rapidly engulf a large volume of prey-laden water at high speed, which they then filter to capture suspended prey. Engulfment biomechanics are mostly governed by the coordinated opening and closing of the mandibles at large gape angles, which differentially exposes the floor of the oral cavity to oncoming flow. The mouth area in rorquals is delimited by unfused bony mandibles that form kinetic linkages to each other and with the skull. The relative scale and morphology of these skeletal elements have profound consequences for the energetic efficiency of foraging in these gigantic predators. Here, we performed a morphometric study of rorqual mandibles using a data set derived from a survey of museum specimens. Across adult specimens of extant balaenopterids, mandibles range in size from ~1–6 m in length, and at their upper limit they represent the single largest osteological element of any vertebrate, living or extinct. Our analyses determined that rorqual mandibles exhibit positive allometry, whereby the relative size of these mandibles becomes greater with increasing body size. These robust scaling relationships allowed us to predict mandible length for fragmentary remains (e.g. incomplete and/or fossil specimens), as we demonstrated for two partial mandibles from the latest Miocene of California, USA, and for mandibles from previously described fossil balaenopterids. Furthermore, we showed the allometry of mandible length to body size in extant mysticetes, which hints at fundamental developmental constraints in mysticetes despite their ecomorphological differences in feeding styles. Lastly, we outlined how our findings can be used to test hypotheses about the antiquity and evolution of lunge feeding. 

ADDITIONAL KEYWORDS: bone – Cetacea – Mysticeti.

## INTRODUCTION

Baleen whales (or crown Mysticeti) are the only known mammalian filter-feeders. Unlike odontocetes, which feed on single prey items, mysticetes process large quantities of prey suspended in water using baleen plates, which allows them to filter large volumes of prey-laden water (Pivorunas, 1979; Werth, 2000; Goldbogen, 2010). A group of baleen whales known as rorquals (crown Balaenopteridae), which include some of the largest vertebrates ever, exhibit a specialized filter feeding mode called lunge feeding.

*Corresponding author. E-mail: pyensonn@si.edu

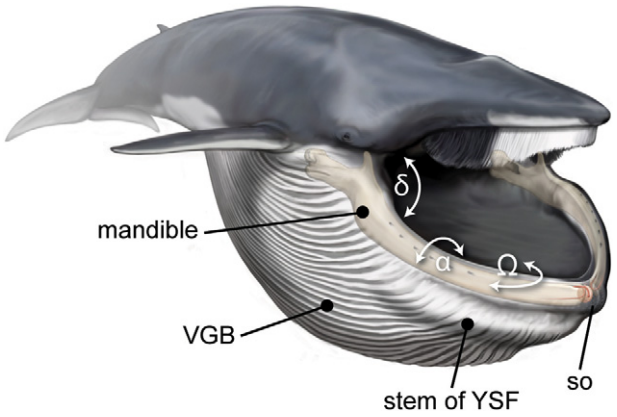


**Figure 1.** Engulfment morphology in balaenopterids, exemplified by a fin whale (*Balaenoptera physalus*), with mandible morphology highlighted by a translucent mask. Mandibles rotate through three axes: delta, alpha, and omega. Abbreviations: so, sensory organ; VGB, ventral groove blubber; YSF, Y-shaped fibrocartilage. Art by C. Buell.

This feeding mechanism involves the engulfment of prey-laden water in a single, rapid gulp (Goldbogen, 2010; Pyenson *et al*., 2012; Fig. 1). During a single lunge, rorqual mandibles rotate through three orthogonal axes, which were defined by Lambertsen, Ulrich & Straley (1995) as follows: delta rotation, or the depression of mandibles; alpha rotation, or the inner or outer roll of the mandible along its main axis; and omega rotation, or right to left yaw of the mandible (Fig. 1). At the apogee of the lunge, the overall gape angle approaches 90° (Brodie, 1993; Brodie, 2001), as a hyper-expandable ventral blubber layer provides an enhanced capacity for the oropharyngeal cavity (Orton & Brodie, 1987).

Because rorqual mandibles exhibit significant curvature, their overall rotation dramatically increases the area of the mouth and the flux of water into the ventral pouch. The integration of such morphological data with kinematic data from animal-borne recording systems has increased our understanding of the mechanics, hydrodynamics and energetics of this unusual feeding mechanism (Potvin, Goldbogen & Shadwick, 2009, 2010; Goldbogen *et al*., 2011, 2012). These studies have demonstrated the crucial role of mandibles in the dynamics of the engulfment process, although it remains unclear how the dimensions of these structures vary across the scale of living and extinct balaenopterids.

Unlike other vertebrates that are capable of similarly large gapes, such as macrostomatan snakes (Vincent *et al*., 2006), balaenopterids feed using mandibles composed of single bony elements, derived from the embryonic dentaries (Mead & Fordyce, 2009: 42). These mandibles are unfused at the distal, mandibular symphysis, a condition that has persisted in mysticetes since the Oligocene (Fitzgerald, 2012; Pyenson *et al*., 2012). Posteriorly, the articular condyles of each ramus are enveloped by fibrous temporomandibular joints (Brodie, 2001) that articulate with the glenoid fossae of the squamosal bones in the skull. These specialized joints dramatically increase the kinetic freedom of the skull, and the manner in which they envelop the entire articular condyle probably accommodates shear forces within the joint during major, rapid excursions of the mandible during a lunge (Brodie, 2001), much like an intervertebral joint (Currey, 2002).

Ventrally, the mandibles are connected by muscles and derived tissues of the floor of the mouth, external to the oral cavity and throat, including the accordion-like ventral groove blubber (Pivorunas, 1977; Lambertsen, 1983). Balaenopterid mandibles also exhibit a prominent, laterally deflected coronoid process, which serves as an attachment point for the temporalis muscle (Brodie, 1993). However, the detailed myology and functional anatomy of the engulfment apparatus remain poorly understood in adult balaenopterids because of the logistical difficulties in accessing, manipulating, and conducting experiments on these taxa. Nonetheless, the mandibles represent key indicators of engulfment performance, as delimiters of the oral cavity, and thus demonstrably have a bearing on lunge-feeding kinematics and energetics (Goldbogen *et al*., 2011).

Balaenopteridae are also abundantly represented in the fossil record, in marine sedimentary rock units from the late Miocene through the Pleistocene, although the taxonomy and systematics of fossil balaenopterids remain work in progress (Deméré, Berta & McGowen, 2005; Bisconti, 2007a; Bisconti, 2010a). Since the mid-19$^{th}$ century, cetacean systematists described many different extinct mysticete genera that share general features with living rorquals, but their phylogenetic relationships remain ambiguous. These 19$^{th}$ century taxa may in fact belong to distantly related lineages, although resolving their systematic position is hindered by non-comparable elements, inaccessible or lost specimens, and ambiguous original diagnoses (Bisconti, 2007b). Extinct balaenopterids described in the late 20$^{th}$ century, such as *Parabalaenoptera bauliensis*, are known from relatively complete skeletal material, including cranial, mandibular, and postcranial elements (Deméré *et al*., 2005). Although the taxonomic membership for many fossil balaenopterids remains unresolved, phylogenetic analyses have recovered some fossil taxa as members of crown Balaenopteridae, lending legitimacy to inferences of lunge-feeding modes in these extinct taxa (Deméré *et al*., 2008).

Such fossil data play important roles in evaluating hypotheses about the evolution of lunge feeding, although much of the available morphological data for balaenopterids (both living and extinct) has not been analysed in a comparative, phylogenetic context.

Given their fundamental importance as a key element in lunge feeding, we undertook a comparative study of balaenopterid mandibles to better understand their scaling properties. We amassed a data set across the size range of nearly all living rorqual species by generating a specimen-based data set that includes mandibles ranging from ~1 to 6 m in length. We quantified the dimensions of rorqual mandibles and used allometric and comparative phylogenetic analyses to assess the scaling of the engulfment apparatus. We then used our allometric equations to predict mandible length for fragmentary fossil balaenopterid mandibles. Furthermore, we compiled a second specimen-based data set to determine mandible scaling relationships among all mysticetes. Lastly, we address the implications of such scaling relationships for filter feeding in these gigantic cetaceans, as well as understanding the antiquity, ecomorphology, and evolution of lunge feeding in rorquals.

## MATERIAL AND METHODS

### Comparative data set

We constructed two data sets for this study: (1) a mandibular data set exclusively using museum specimens (regardless of attendant body size data); and (2) a broader data set, including mandibular measurements and total length (TL) data from museum specimens. Measurements and museum specimens are listed in Appendix S1.

For the first data set, we collected data from 34 individual specimens of living balaenopterids, comprising six species: *Balaenoptera acutorostrata*, *Balaenoptera borealis*, *Balaenoptera edeni/brydei*, *Balaenoptera musculus*, *Balaenoptera physalus*, and *Megaptera novaeangliae* (see Appendix S1). The resultant data set thus included the full size range of extant balaenopterids, including neonatal specimens of *B. acutorostrata*. Although we did not sample *Balaenoptera bonaerensis* and *Balaenoptera omurai* because of their extreme rarity in museum collections, these size categories were represented by closely related species (*B. acutorostrata* and *B. edeni/brydei*, respectively). Adult TL for *B. bonaerensis* is slightly larger than *B. acutorostrata* (Konishi *et al.*, 2008), but the specimens of the former were unavailable for study. We also note that we considered the allometry of *B. brydei* to effectively represent the same as *B. edeni*, despite the phylogenetic status of these poorly established taxa (Sasaki *et al.*, 2006; Kato & Perrin, 2009). For the first data set we restricted one subset of regression analyses to include subadult to adult (mature) specimens only; another subset of regression analyses included all mature, juvenile, and neonatal specimens. Skeletal maturity for mandibles was largely assessed by the condition of the bone surface (i.e. smooth in mature individuals), attendant voucher data, and whether TL was congruent with reported mature values from previous literature (e.g. Pyenson & Sponberg, 2011). Because mandibles undergo intramembranous ossification (Drake, Vogl & Mitchell, 2010), we could not use other ontogenetic metrics available for balaenopterid osteology (e.g Walsh & Berta, 2011).

For the second data set, we collected data from 59 individual specimens of 11 species of living mysticetes, except for the aforementioned omissions. This second data set included mandibular length measurements and TL data (Mackintosh & Wheeler, 1929) that were recorded with the vouchers. Its taxonomic scope comprises all extant families of mysticetes. As with the first data set, we restricted the sample to subadult to adult specimens only.

Collecting morphometric data from osteological collections of large cetaceans presents several logistical challenges. Large cetaceans are rarely curated in museum collections with attendant natural history data (i.e. provenance, condition, sex, and ontogenetic stage), and the large size of their skeletal remains (> 6 m in length; > 500 kg in total, dry weight; see Discussion) make museum voucher specimens difficult to clean, store, and access for detailed examination and measurement (True, 1904). Second, extant balaenopterid diversity is not equally represented in museum collections, necessitating extensive travel to collect data from immovable specimens. Lastly, to generate a sufficient sample size for this study, we included specimens that lacked attendant size data (the first data set) as well as those that were collected from individuals with known TLs (the second data set). Although such data are relevant for many morphological investigations, TL is inconsistently represented in the accessioned remains of most cetaceans stored in natural history collections (see Pyenson & Sponberg, 2011: 271–272).

### Measurements

For mandibular measurements (Fig. 2), we reported curvilinear and chord lengths for right or left mandibles, or, when both were present, we calculated the mean. Curvilinear lengths (Cu) followed the ventral margin of the mandibles from their anteromedial termination near the gnathion, ventral to the symphyseal surface, and extending to the posterior apex of the angular condyle. The keeled ventral margin

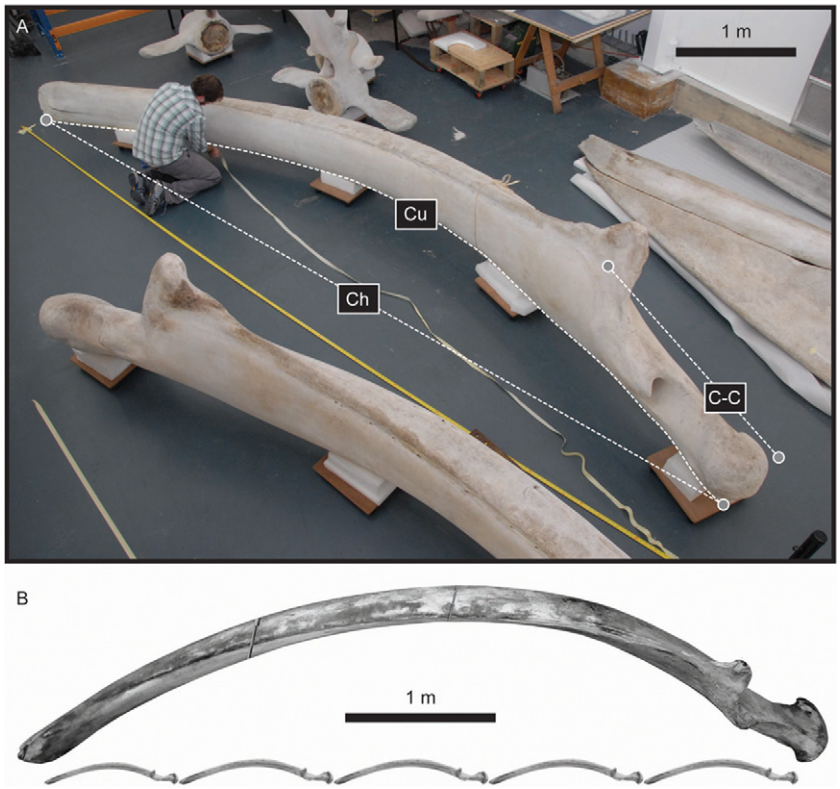


**Figure 2.** A, mandible length measurements for CM Ma 608, an adult blue whale (*Balaenoptera musculus*). Chord length (Ch), curvilinear length (Cu), and the distance from the coronoid process to the articular condyle (C–C) were either measured as illustrated, collected from the literature, or measured in ImageJ; see Material and methods for further description. Photograph by R.E. Fordyce. B, composite photo of a mandible from an adult *B. musculus* (LACM 72562), representing the upper size limit in mysticetes (chord length = 5.13 m), versus the mandible of an adult minke whale (*Balaenoptera acutorostrata*; MVZ 134463), representing the smallest size of extant rorquals (chord length = 1.02 m).

along most of the mandibular ramus length provided a consistent landmark for measuring curvilinear length, although this measurement is inconsistently explained in the literature. Chord lengths (Ch) represent the straight-line distance between the anteriormost and posteriormost points. Because many fossil balaenopterid mandible specimens are fragmentary, we used a measurement that is usually preserved on incomplete, but taxonomically diagnostic mandibular material. This measurement, termed C–C, was measured as the linear distance from the articular condyle to the midpoint of the coronoid process, along the corpus of the mandible, which Bisconti (2010a, b) described as the condyle–coronoid distance. Measurements were collected directly from the specimens or, when necessary, from images digitized with a scale bar using ImageJ (Rasband, 2012).

### Institutional abbreviations

CASG, Department of Invertebrate Zoology and Geology, California Academy of Sciences, San Francisco, California, USA; CM, Canterbury Museum, Christchurch, New Zealand; LACM, Natural History Museum of Los Angeles County, Los Angeles, California, USA; MB, Museum für Naturkunde, Berlin, Germany; SBAER, Inventory of the Soprintendenza per i Beni Archeologici dell'Emilia Romagna at the Museo Paleontologico di Salsomaggiore Terme, Italy; MVZ, University of California Museum of Vertebrate Zoology, Berkeley, California, USA; UBC, University of British Columbia Beaty Biodiversity Museum, Vancouver, British Columbia, Canada; UCMP, University of California Museum of Paleontology, Berkeley, California, USA; USNM, Department of Vertebrate Zoology, National Museum of Natural History, Smithsonian Institution, Washington, DC, USA (see Appendix S1 for institutional abbreviations from other specimens in the data sets).

### Bivariate linear regressions

We regressed the curvilinear and chord lengths against C–C for our first data set of extant

balaenopterid mandibular measurements. Right and left measurements from individual specimens were averaged and then the data were log-transformed. We conducted bivariate ordinary least squares (OLS) lineage regressions (McArdle, 1988) for three versions of this data set: all specimens; species values (means for all mature specimens); and independent contrasts for species values, which used intraspecific means. To determine differences between correlations of C–C with Cu and Ch, we compared the slopes of the lines from both bivariate plots, which was essentially equivalent to an *F*-test.

### Phylogenetic independent contrasts

In comparative biology, values for taxonomic data are not independent; instead, they are related to one another by history, as indicated by phylogenetic relationships (Garland, Harvey & Ives, 1992; Garland & Ives, 2000). Phylogenetic comparative methods provide a robust set of tools to assess how phylogeny impacts relationships for traits among taxa that are related to one another by different phylogenetic hypotheses (i.e. phylogenetic trees). Among various approaches, we examined correlated trait evolution in our data sets using phylogenetically independent contrasts (PICs; Felsenstein, 1985). We calculated these contrasts using log-transformed data entered into MESQUITE 2.6 (Maddison & Maddison, 2011) with the phenotypic diversity analysis program module (PDTREE), with all branch lengths set to 1.0 (Midford, Garland & Maddison, 2005). Among the available mysticete phylogenies, we based our balaenopterid topology (for the first data set) on a previously published molecular tree (Sasaki *et al*., 2005), pruning it to the six balaenopterid species that we sampled. Recent molecular studies (McGowen, Spaulding & Gatesy, 2009; Steeman *et al*., 2009) reveal congruent relationships among these six taxa, although not for other unsampled taxa (e.g. *B. omurai*) (Marx, 2011). For the second data set, we used a consensus tree for 11 species of mysticetes, the structure of which most closely parallels that of Sasaki *et al*. (2005: fig. 5). Again, as with the balaenopterid consensus tree, the mysticete consensus tree places *Eschrichtius* in a polytomy with other Balaenopteridae, rendering this clade potentially paraphyletic; *Caperea* is sister to this latter polytomy, with Balaenidae as the basal group. All other subclade relationships are uncontroversial among the 11 species sampled herein. Plots of phylogenetically correct (OLS) regression and associated confidence intervals were then mapped onto the original tip data space (Garland & Ives, 2000).

### Fossil data

We incorporated fossil balaenopterid data into this study in two ways. First, subsequent to the regression analyses, we plotted measurements from the complete mandibles belonging to known fossil balaenopterids. After a survey of known taxa, we selected *Plesiobalaenoptera quarantellii* (SBAER 240505) and *Parabalaenoptera bauliensis* (CASG 6660) from the late Miocene of northern Italy and northern California, respectively. Second, we applied predictive equations to estimate the size of fragmentary fossil balaenopterid mandibles not included in the aforementioned data sets. These incomplete specimens derive from three specimens: the partial mandibles belonging to '*Megaptera*' *hubachi* (MB.Ma. 28570), a fossil balaenopterid putatively from the late Miocene of Chile; and isolated, partial mandibles from two separate localities of the Purisima Formation, in central California, USA (Figs 3, 4). The mandibles of '*M.*' *hubachi* are reconstructed with plaster to give the impression of being complete (Dathe, 1983), although Bisconti (2010b) clarified that the posterior ~25% are


**Figure 3.** Examples of partial fossil balaenopterid mandibles. A, UCMP 81001, referred to Balaenopteridae; B, UCMP 194914, also referred to Balaenopteridae. Note that both specimens are incomplete, lacking anterior or distal portions. Abbreviations: an, angular process; ar, articular process; cp, coronoid process; mc, mandibular corpus; mf, mandibular foramen; ptf, pterygoid fovea.

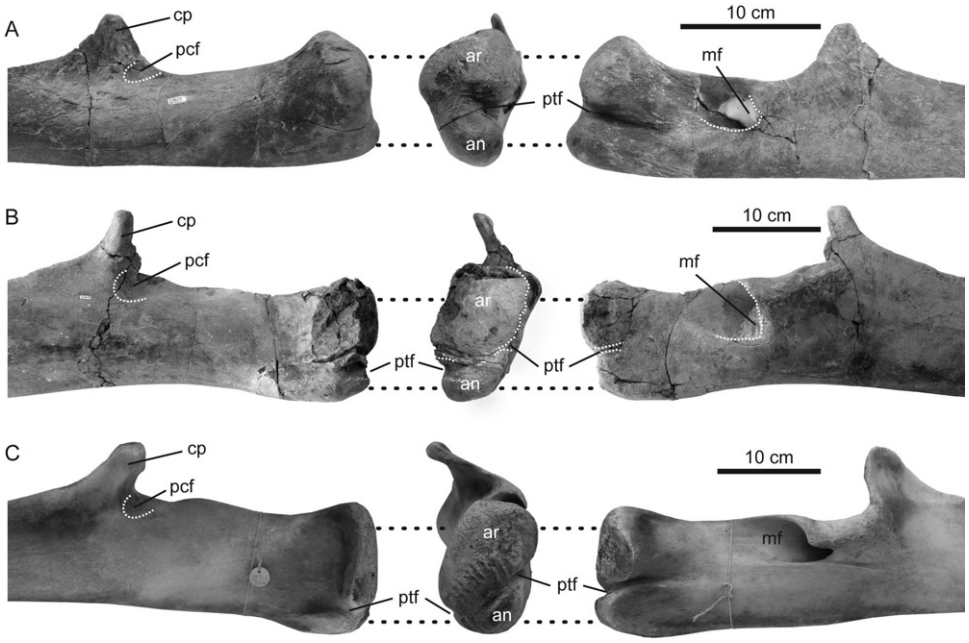


**Figure 4.** Comparative morphology of proximal (i.e. posterior) ends of fossil and extant balaenopterid mandibles: from left to right, lateral, posterior, and lingual views of the proximal mandible. A, UCMP 81001, fossil specimen referred to Balaenopteridae; B, UCMP 194914, fossil specimen also referred to Balaenopteridae; C, living *Balaenoptera acutorostrata*, composite views from the right and left mandibles of MVZ 126873. All specimens are scaled to approximately the same C–C distance. Abbreviations: an, angular process; ar, articular process; cp, coronoid process; mf, mandibular foramen; pcf, postcoronoid fossa; ptf, pterygoid fovea.

real, including all of the morphology along the C–C distance. The first isolated specimen, UCMP 81001, represents an incomplete, proximal left mandible (Figs 3A, 4A), which was collected from exposures of the Purisima Formation along Drakes Beach, in the Point Reyes National Seashore, Marin County, California, USA, at UCMP locality V6858 (Barnes, 1976). The sea cliffs along Drakes Beach preserve sections of late Neogene marine units that Galloway (1977) referred to Drakes Bay Formation. Clark *et al*. (1984) correlated the upper units of Drakes Bay with lithologically similar rocks of the Purisima Formation, much further south along the San Andreas Fault, in Santa Cruz County, California (Clark *et al*., 1984). Here, we follow their determination in referring to the sequence of rocks above the basal glauconitic greensand along Drakes Beach as the Purisima Formation.

The second specimen, UCMP 194914, represented by an incomplete right mandible (Figs 3B, 4B), originates from the Opal Cliffs locality (UCMP locality V6875), in the city of Santa Cruz, Santa Cruz County, California, USA. Opal Cliffs is one of many localities of the Purisima Formation exposed along the sea cliffs in Santa Cruz (Powell *et al*., 2007). These sandstone exposures have produced an abundance of fossil marine mammal material, although much of it is incomplete and fragmentary. Based on similar relationships, lithologies and fossil content between the Drakes Bay Formation and rock units in San Mateo County, California, Clark *et al*. (1984) correlated the lower greensand unit of the Drakes Bay Formation with the Santa Margarita Formation in San Mateo County. Clark *et al*. (1984) also correlated the overlying mudstone unit with the Santa Cruz Mudstone, and the uppermost unit with the Purisima Formation. Although correlating fault-bounded rocks at a regional level is difficult, Powell and Powell *et al*. designated the upper units of Galloway's (1977) Drakes Bay Formation as the Purisima Formation (Powell, 1998; Powell *et al*., 2007).

## RESULTS

### Allometry of balaenopterid and mysticete mandibles

Scaling relationships of total mandible length versus the distance from the articular condyle to the coronoid process (C–C) were positively allometric (Fig. 5), as well as being significantly correlated ($P < 0.001$; $R^2 = 0.97$). Overall, C–C decreased with larger mandible lengths (slope = 1.23 and 1.24, for both Cu and Ch lines, respectively), indicating that the position

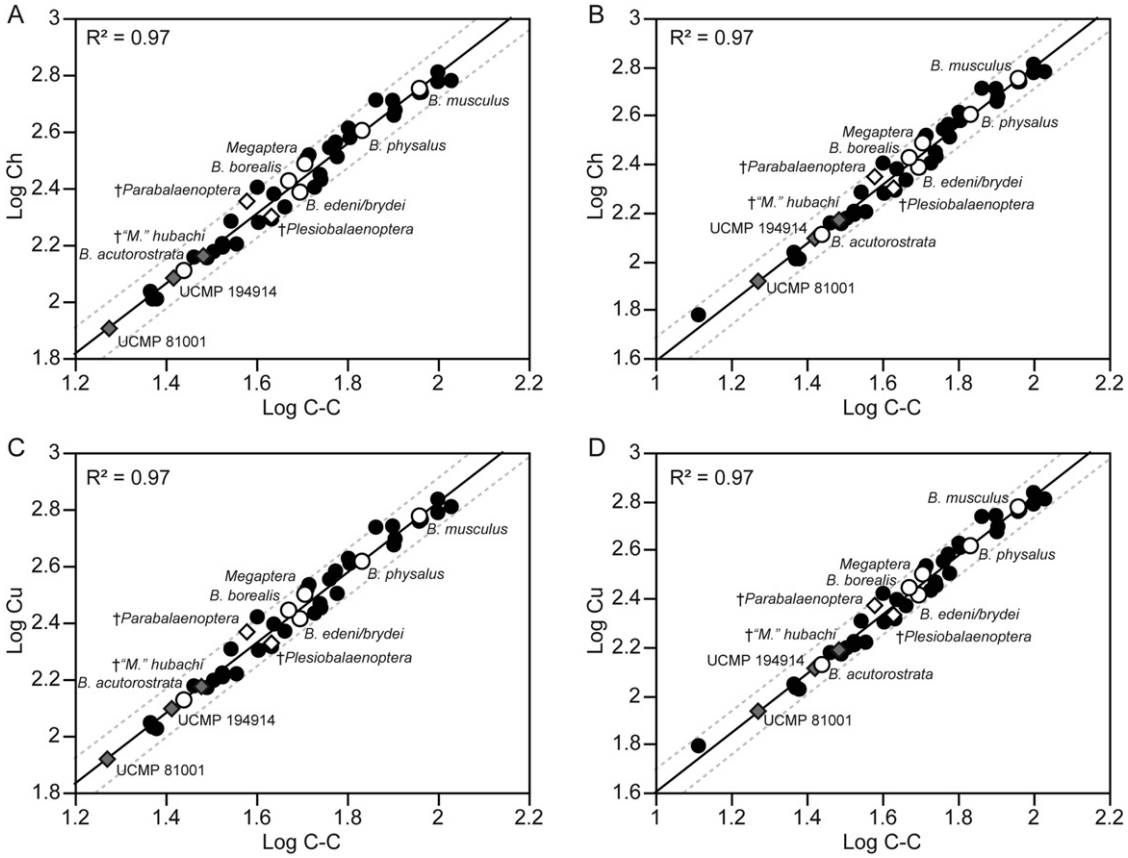


**Figure 5.** Allometric relationships of balaenopterid mandibles using different linear measurements. Chord length (Ch) versus the distance between the coronoid process and the articular condyle (C–C): (A) mature specimens only; (B) both immature and mature specimens. Curvilinear length (Cu) versus the distance between the coronoid process and the articular condyle: (C) mature specimens only; (D) both immature and mature specimens. Black dots represent extant specimens, and white circles represent extant species means. Dotted and solid lines represent 95% confidence intervals and slopes, respectively. Grey diamonds represent partial fossils with C–C values, and open, white diamonds represent complete fossils, both plotted after regressing extant data. See text for statistical results.

of the coronoid process in larger balaenopterids is located further posteriorly than in smaller balaenopterids. We included two metrics of mandible length in our analysis (Cu and Ch), and we found no statistical difference between the slopes of their lines. Our bivariate plots included all specimens ($n = 34$), as well as species averages, for the six species assessed (Fig. 5). To assess the phylogenetic underpinnings of these scaling relationships, we regressed the PICs of these bivariate plots, mapped back onto original data space (Garland & Ives, 2000). In this analysis, both Cu and Ch exhibited the same scaling relationships, indicating that phylogeny had no effect on rorqual mandible scaling (see Appendix S1). For some taxa (e.g. *B. acutorostrata*), we included neonatal and juvenile specimens within the first data set to evaluate the role of early ontogeny. Interestingly, the presence of these specimens did not change the allometric results presented herein (Fig. 5B, D).

Plotting fossil values for C–C from the fossil specimens reported herein revealed that some fossil balaenopterids possessed mandible lengths smaller than the adult mandibles of the smallest extant balaenopterids in this data set, *B. acutorostrata*. Following equations from the slope of the line for Ch versus C–C, using mature specimens, we estimate that UCMP 81001, 194914, and '*M.*' *hubachi* possessed complete mandibles that measured approximately 0.82, 1.23, and 1.45 m, respectively, in chord distance (see calculations in Appendix S1). The calculated chord length for '*M.*' *hubachi* is slightly less than the estimated length of 1.57 m published by Bisconti (2010b: table 1).

Our second data set examined the relationship between mandible length (Ch) and TL across nearly all species of living mysticetes (Fig. 6; Table 1). We determined that Ch scaled closely with TL ($P < 0.001$; $R^2 = 0.94$), and its slope (0.87) deviated from isometry.

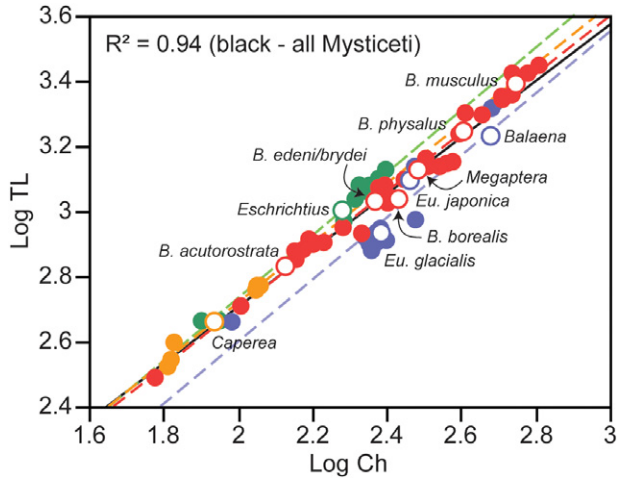


**Figure 6.** Bivariate plot of body size (total length, TL) against mandible length (chord length, Ch) across living mysticetes. The solid black line represents the slope of all data combined, and white circles represent extant species means. Key: *Caperea*, gold; *Eschrichtius*, green; Balaenidae, purple; Balaenopteridae, red. See Appendix S1 for regression results.

**Table 1.** Ratio of mandible length (Ch, or chord length) to body size (TL, or total length) in extant mysticetes, supported by data from museum specimens in this study

| Clade | Taxon | Ch : TL | *N* |
|---|---|---|---|
| Eschrichtiidae | *Eschrichtius robustus* | 0.19 | 11 |
| Neobalaenidae | *Caperea marginata* | 0.19 | 3 |
| Balaenopteridae | *Balaenoptera acutorostrata* | 0.20 | 8 |
| Balaenopteridae | *Balaenoptera edeni* | 0.22 | 4 |
| Balaenidae | *Eubalaena glacialis* | 0.23 | 3 |
| Balaenopteridae | *Balaenoptera musculus* | 0.23 | 6 |
| Balaenopteridae | *Balaenoptera physalus* | 0.23 | 4 |
| Balaenopteridae | *Balaenoptera borealis* | 0.23 | 4 |
| Balaenopteridae | *Megaptera novaeangliae* | 0.25 | 4 |
| Balaenidae | *Eubalaena japonica* | 0.28 | 1 |
| Balaenidae | *Balaena mysticetus* | 0.28 | 9 |

*N*, number of specimens per taxon.

As with the first data set, PICs of this second data set produced no discernible difference (slope = 0.88; $R^2 = 0.94$; see Appendix S1), which likewise suggests that the scaling of mandible length with body size in living mysticetes is independent of phylogeny (but see Discussion). Because the inclusion of neonatal and juvenile specimens in this first data set did not change the allometric results, we included juvenile specimens in this second data set to increase sampling.

### Reconstructed total length for fossil Balaenopteridae

Conducting a regression analyses on the second data set allowed us to develop balaenopterid-specific equations for predicting body size using mandible measurements of museum specimens (see calculations in Appendix S1 based on balaenopterid Ch and TL data). Based on its smooth bone surface, we argue that UCMP 81001 probably represents a subadult to mature individual, despite its small size (estimated TL = 3.26 m). We estimate that UCMP 194914 belonged to an individual with a TL of 4.83 m, which was larger than an adult *Caperea*, but smaller than an adult *B. acutorostrata* (Fig. 6). By contrast, we estimate TLs of '*M.*' *hubachi*, *Parabalaenoptera*, and *Plesiobalaenoptera* as 5.62, 7.70, and 8.54 m, respectively, which are all specimens based on mature individuals, and fall within the size range for extant balaenopterids (Fig. 5).

### Diagnosis and ages of fossil Balaenopteridae

Both partial fossil mandibles reported here are assigned to Balaenopteridae on the basis of a suite of morphological features that they share with extant balaenopterid mandibles, to the exclusion of other mysticetes. This suite of features includes: an elevated, finger-like, and laterally deflected coronoid process (Lambertsen *et al.*, 1995; Bouetel, 2005); a posteriorly directed and hemispherically shaped articular condyle that is separated from a comparatively smaller, angular process by a pterygoid fovea (Bisconti, 2010b); and a relatively small, tubular bony aperture for the mandibular foramen (Zeigler, Chan & Barnes, 1997; Deméré *et al.*, 2005; Steeman, 2007). Both fossils also have a reduced postcoronoid fossa (see Bisconti, 2010a: 952, for a discussion), relative to the elevated crest observed in more basal, fossil mysticetes, such as *Aglaocetus* or *Pelocetus*. Other non-balaenopterid taxa possess some of these aforementioned characters, but only balaenopterids possess the entire suite.

One of the fossils used in the analysis, UCMP 194914, compares favourably with extant balaenopterids in the shape and deflection of its coronoid process. Also, UCMP 194914 has an articular condyle that is proportionally larger than its angular condyle, which has a surface that broadens and is exposed posterolaterally, and which is separated from the angular condyle by a clear pterygoid fovea (*sensu* Bisconti, 2010b) that rings the posterior end of the mandible from lateral to medial sides. UCMP 194914 shares strong overall similarities in lateral profile with the fossil taxa '*M.*' *hubachi* and *Plesiobalaenoptera*, but it is unlike *Parabalaenoptera*, which has a

higher and more gradually sloping anterior margin to the coronoid process.

Notably, UCMP 81001 has a pterygoid fovea that extends only from the medial side of the proximal end of the mandible to the posterior side. In contrast, all extant balaenopterids (and many putative fossil balaenopterids) exhibit a clear division between the articular and angular condyles, with a clear pterygoid fovea that extends from the lateral surface all the way to the medial surface. The dorsoventral height of the coronoid process (from the ventral margin of the mandibular corpus) is close to the same height of the angular and articular condyles, which contrasts with most other extant balaenopterids and UCMP 194914. Lastly, the aperture of the mandibular foramen in UCMP 81001 is similar to that of some fossil balaenopterids, especially *Plesiobalaenoptera*. Although UCMP 81001 possesses hallmark balaenopterid traits, it probably belonged to an extinct, and presently unknown, balaenopterid taxon.

Overall, both of these fossils from the Purisima Formation in California are largely coeval. In Marin County, K/Ar dates of 7.9 ± 0.3 Mya from a glauconitic greensand unit down-section from UCMP V6858 (Clark & Brabb, 1997) constrains the age of UCMP 81001 to the latest Miocene; the top of the Purisima Formation in Marin County is probably early Pliocene in age (Galloway, 1977). Similarly, in Santa Cruz County, Powell *et al*. (2007) argued that the consensus of biostratigraphic and geochronological evidence indicated a latest Miocene to late Pliocene age for the Purisima Formation in this area, and thus for UCMP 194914. Powell *et al*. (2007) also indicated that the base of the Purisima Formation along the sea cliffs of Santa Cruz is geochronologically constrained by a K/Ar date of 6.9 ± 0.5 Mya (Madrid, Stuart & Verosub, 1986), which establishes the maximum age of the Purisima Formation in Santa Cruz County as latest Miocene. Thus, the fossil balaenopterid specimens reported herein are latest Miocene to early Pliocene in age (~6–5 Mya).

## DISCUSSION

We undertook this comparative study of balaenopterid mandible allometry because mandibles play a fundamental role in delimiting the size of the oral cavity in lunge feeding. Our allometric analyses of simple mandible dimensions, across the size range of all living rorqual species, demonstrated a strong and significant scaling relationship among functionally relevant features (i.e. C–C and Ch). In the first case, we used the allometric relationships to estimate the original size of fragmentary fossil balaenopterid mandibles. In the second case, we explored how mandibles in all other mysticetes scale with body size. Below, we elaborate on the significance of these results, and expand on key points that hold promise for future work on the biomechanics and evolution of rorqual lunge feeding.

### Mandible scaling and lunge-feeding biomechanics

As an integral component of the craniomandibular apparatus, mandibles play an important role in lunge-feeding mechanics. These features include: the perimeter of the oral cavity and thus engulfment volume (Goldbogen, Pyenson & Shadwick, 2007; Goldbogen, 2010; Goldbogen *et al*., 2011); the large gape angles, which rely on a flexible temporomandibular joint (Brodie, 1993, 2001); and the lateral rotations of the bowed rami, which can adjust the articulation of the jaws with the rostrum independently on the right and left sides (Lillie, 1915; Lambertsen *et al*., 1995). Notably, Goldbogen *et al*. (2007), Goldbogen, Potvin & Shadwick (2010), Goldbogen *et al*. (2011), and Potvin *et al*. (2009, 2010) used mandible measurements to model mouth area, and estimate engulfment volume and engulfment mechanics in different species of rorquals. However, the specific physical forces at play during the engulfment process remain poorly understood in an empirical way because of the logistical and legal barriers in dealing with large marine vertebrates such as rorquals. Although adult rorquals were the targets of sustained hunting in the early through to the late 20th century (Reeves & Smith, 2006), our understanding of their basic craniomandibular anatomy is deficient in specifics about joint articulations and basic morphometrics, which excludes the possibility of using standard approaches for analysing feeding biomechanics in marine vertebrates (Westneat, 2004). These aforementioned challenges in large part affected our original intention to record simple measurements of rorqual mandibles, especially using a data set grounded in vouchered museum specimens, instead of secondary or tertiary literature.

Our analyses, with the first data set, demonstrated that the position of the coronoid process (primary point of attachment for the temporalis muscle) along the length of the mandible is relatively closer to the condyle in larger rorquals (Fig. 5). This finding suggests that mechanical advantage (Currey, 2002), when closing the mandibles against drag to complete a single lunge, is also comparatively lower in larger rorquals. Reduced mechanical advantage, however, may be ameliorated in larger rorquals because they exhibit longer time scales during engulfment, and thus relatively lower peak drag forces (Potvin *et al*., 2010). Given the small body sizes of fossil rorquals, the even higher mechanical advantage of these

diminutive, extinct balaenopterids may have been important in the evolution of lunge feeding. Specifically, it is possible that the earliest form of lunge feeding, which probably occurred at small body sizes, involved largely rapid single gulps, a mode that was later elaborated at larger body sizes with less biomechanically advantageous mandibles but for larger and longer gulps. Future modelling work, using parachute physics as an analogy (e.g. Potvin *et al*., 2009, 2010), may be fruitful in clarifying this possible evolutionary scenario.

It is important to note that the simple linear measurements used in this analysis vastly oversimplify the complex morphology of the posterior end of the rorqual mandible. There are clear morphological differences between the size extremes observed in balaenopterids: for example, in lateral view, the coronoid process in *B. actutorostrata* is narrow and spatulate (Fig. 4C), whereas it has a broad, sloping base in *B. musculus* (Fig. 2A, B). Equally, in medial view, the margin of the articular condyle in *B. acutorostrata* points posterodorsally, whereas the articular condyle in *B. musculus* is depressed and nearly extends ventrally relative to the corpus of the mandible. These differences underscore two important needs for future investigations: (1) more detailed, comparative descriptions of the mandibular morphology across all balaenopterids, including fossil taxa; and (2) clarification about the relationship between soft tissue structures (e.g. insertion of the temporalis and pterygoid muscles) and their bony tissue correlates (e.g. the size and shape of the coronoid process and the pterygoid fovea), especially for adult balaenopterids. The latter issue will require broader comparative studies in osteological collections with sufficient samples to understand latent variation; the former issue will require unique opportunities to dissect the craniomandibular apparatus of these gigantic cetaceans (e.g. see Pyenson *et al*., 2012).

The near-isometric scaling of mandibles relative to body size across all mysticetes (Fig. 6) was a surprising finding, given the disparity among filter-feeding modes in extant mysticetes (Werth, 2000). Our analyses with the first data set demonstrated that the inclusion of juvenile (even neonatal) specimens did not significantly change the allometric slopes of relationships within Balaenopteridae (see Fig. 5B, D). This uniformity in scaling indicates that the morphological bauplan for mandibular scaling is set late *in utero*, hinting at the dominant role of developmental constraint in shaping the functional morphology of balaenopterids. Our analyses of mandible scaling relative to body size in all extant mysticete lineages (Fig. 6), which included juvenile and immature specimens, showed similar slopes, ranging in coefficients from 0.89–0.95 across family-level groupings (all of which were significant; see Appendix S1). This latter finding suggests that the pattern of ontogenetic mandibular scaling in balaenopterids may also extend across all mysticetes, despite different feeding modes. In turn, these allometric data suggest that scaling relationships of the feeding apparatus in baleen whales might have been set at the origin of crown Mysticeti.

Balaenids had the largest mandibles relative to body size (Table 1), with the upper limit of the ratio reaching nearly 0.30, providing much needed quantitative data for the oft-cited claim that balaenids have an oral cavity that is one-third their body length (e.g. Lambertsen *et al*., 1995). However, it is important to note, in this specimen-based data set, that one species of balaenid, *Eubalaena glacialis* (North Atlantic right whales) had a ratio similar to that of balaenopterids. This unusual finding is not affected by ontogeny, as juvenile and adult specimens (LACM 54763 and USNM 257513, respectively) both had similar ratios (0.20–0.23; see Appendix S1). Rorquals had ratios closer to 0.20–0.25, with *Megaptera* possessing a ratio of 0.25. Interestingly, *B. acutorostrata* shared ratios close to that of *Eschrichtius* (the sister taxon to Balaenopteridae) and *Caperea*, despite divergent feeding modes and craniomandibular morphologies (Werth, 2000). These mandibular proportions simplify far more complex ecomorphological patterns that are related to the skull (see Goldbogen *et al*., 2010), and a deeper understanding of the variation of these features in balaenopterids requires coupling mandibular and skull measurements in future work.

### Size extremes for bony elements

As a single osteological element, the mandibles of the largest balaenopterids (e.g. *B. musculus* or blue whales) are unequivocally the largest single osteological element for any vertebrate in the history of life, an observation that can be attributed to Pivorunas (1977: 299). No single osteological element from any other vertebrate, living or extinct, compares in terms of linear dimensions and weight. Weights for balaenopterid mandibles derive from industrial whaling reports, although some reports fail to clarify the distinction between single dentaries and conjoined dentaries in a mandible (using more traditional nomenclature; see Mead & Fordyce, 2009: 42). For example, Laurie (1933: 403–404) reported 'jaw bones' of a 20.30-m blue whale weighing 928 kg, whereas a 'jaw bone' from a 27.18-m blue whale weighed 2117 kg. Nonetheless, these estimated weights compare favourably with weights recorded for specimens in our data set (e.g. 550 kg dry weight recorded for the right mandible of UBC 17999). To our knowledge, the largest single specimen represented in

extant museum collections are the 6.8-m (in curvilinear length) mandibles of a female *B. musculus* with a TL of 28.0 m, collected from the Southern Ocean in 1939 (USNM 268731). Winston (1950: 395) reported a 6.96-m mandible from a 27.13-m female *B. musculus* (metric conversions from the source data), although no voucher material was reported and it is unknown if any voucher material from this era of Japanese Antarctic whaling has survived. Because pelagic industrial whaling in the Southern Ocean decimated the largest individual *B. musculus* prior to the 1950s (Small, 1971), we suspect that USNM 268731 represents one of the largest examples for the currently available *B. musculus* museum specimens anywhere in the world.

Linear measurements presented herein are unrivaled by the largest elements from terrestrial mammals or sauropod dinosaurs, which rank as contenders in this category; individual postcranial elements do not rank close to this size category, and cranial and mandibular elements of other candidate vertebrates are composed of multiple elements. For example, many extinct marine diapsids (e.g. mosasaurs, ichthyosaurs, and pliosaurs) possess mandibles greater than 1 m in length; and these mandibles are also composed of multiple individual bones. Despite the large absolute size of balaenopterid mandibles, mandibles are not technically long bones, but are actually flat bones that undergo direct, intramembranous ossification, like other cranial bones (Currey, 2002). It remains an open question as to whether this kind of developmental pathway promotes the extreme size growth observed in rorqual mandibles; conversely, few authors have identified clear developmental or evolutionary limits that would prevent mandibles from attaining extreme sizes, with the obvious exception of their use in (near-) weightlessness under water. Nonetheless, we foresee future allometric analysis focusing on direct comparisons between rorqual mandibles and traditional long bone scaling studies (Bertram & Biewener, 1992; Garcia & da Silva, 2004), as well as their densiometry and bending mechanics (Field *et al*., 2010).

### Paleobiological and comparative applications

Many reported fossil balaenopterids are fragmentary or are represented by undiagnostic material (Deméré *et al*., 2005; Bisconti, 2007a, b, 2009, 2010a, b). Indeed, most of the diagnostic balaenopterid fossil record consists solely of cranial material, which is rarely associated with corresponding mandibular elements. In this way, functional inferences about feeding behaviour are severely limited for extinct balaenopterids. In contrast, the occurrence of isolated mandibular elements does provide very clear evidence for ecomorphology and the probable functional aspects of the feeding apparatus (Bisconti & Varola, 2000, 2006). In this study, we have extended Bisconti & Varola's (2000) suggestion for reconstructing mandible length on a partial, fossil mandible using extant data. As a result, we have demonstrated the utility of a strong scaling relationship for estimating the original length of partial mandibles. Because mandible length essentially mirrors skull size in mysticetes (Fig. 5; Table 1; and see Goldbogen *et al*., 2010), we used the strong correlation between condylobasal length and total length in living balaenopterids (see also Pyenson & Sponberg, 2011) as a basis for estimating the size of extinct balaenopterids represented by incomplete material.

Interestingly, in adopting our methods for fossil balaenopterids, we recovered surprisingly comparable size estimates. *Parabalaenoptera*, the holotype and only known specimen of which does not preserve TL, produces similar results to those of Pyenson & Sponberg (2011: table 4), with a calculated TL of 8.54 m (see Appendix S1) from the measured Ch of the complete right mandible. This value is slightly smaller than the best estimate of TL (8.85 m) presented by Pyenson & Sponberg (2011), which used a phylogenetically informed equation that included data from several skull measurements. '*Megaptera*' *hubachi*, a fossil balaenopterid that does not belong in the genus *Megaptera* and probably represents a separate, extinct genus, is represented by a single specimen that is almost complete. Dathe (1983: 844) and Bisconti (2010b) reported a length of the total skeleton of 6.00 m, which is slightly larger than our estimated value of 5.63 m. For the partial fossils represented solely by mandibles, their estimated sizes represented adult balaenopterids below the lower limit of adult total length in extant balaenopterids, suggesting that some of these extinct taxa were smaller than those alive today.

Previously, Lambertsen *et al*. (1995) argued that the acquisition of morphological specializations associated with lunge feeding played a key role in the evolutionary diversification of balaenopterids. Given the preliminary results presented here for two fossil balaenopterids, considered alongside other late Miocene balaenopterids discussed by Deméré *et al*. (2005) and Bisconti (2010b), we argue that that the necessary bony specializations were acquired at least by the late Miocene, and at size ranges below the threshold for living taxa (Pyenson & Sponberg, 2011). Moreover, the stratigraphic and geological contexts of their occurrences provide critical data for informed conclusions about the antiquity of balaenopterids. Such work, especially with specimen-based data sets, should form the basis of future fossil calibrations of phylogenetic trees, in accordance with the guidelines

proposed by Parham *et al*. (2012). Taken together, these different kinds of data sets for extant and fossil balaenopterid data will better test potential evolutionary scenarios for the origin of lunge feeding.

## CONCLUSIONS

Rorqual whales provide data on the upper limits of scaling relationships that underpin many fundamental processes in vertebrate and mammalian physiology, ecology, and evolution. Their large size directly relates to their lunge-feeding performance, a feeding style that efficiently maximizes their ability to access dense aggregates of prey. As a single bony element, rorqual mandibles ultimately constrain the volume of prey-laden water that rorquals engulf while lunge-feeding. Here, we demonstrated that rorqual mandibles are positively allometric, where larger whales exhibited relatively longer mandibles. Such a trend suggests that relative engulfment capacity increases with body size, a feeding characteristic that plays a fundamental role in influencing prey preference, ecological niche, and foraging efficiency. These results are consistent with previous morphometric and functional analyses across differently sized rorquals that suggest a set of limiting factors controlling the upper limit of body size in rorquals. Lastly, the strong scaling relationships of rorqual mandibles demonstrated here can be used to estimate the original length in fragmentary museum specimens, including those of partial fossil balaenopterid mandibles. The ability to reconstruct morphometric data for key fossil taxa, and the integration of those data with extant taxa into comparative phylogenetic analyses, is paramount for understanding the evolution of body size and specialized feeding modes in baleen whales.

## ACKNOWLEDGEMENTS

We thank E. M. G. Fitzgerald, A. Werth, and an anonymous reviewer for diligent, insightful, and constructive comments that improved the quality of this article. For their assistance with museum collections under their care, we thank: M. Flannery, B. Simison, J. DeMouthe, and S. Mansfield (all CAS); S. Stollman (CM); D. Casper and S. Davenport (both Long Marine Laboratory); the staff at the Whale Interpretive Centre, Telegraph Cove, British Columbia; J. Dynes and D. Janiger (both LACM); C. Conroy (MVZ); A. van Helden (Te Papa Tongarewa National Museum of New Zealand); E. M. G. Fitzgerald (Museum Victoria); K. A. Fahy (Santa Barbara Museum of Natural History); E. Rickett, W. Maddison, and A. Trites, (all UBC); P. A. Holroyd (UCMP); C. W. Potter and J. G. Mead (both USNM); and J. Bradley (Burke Museum of Natural History and Culture). For additional logistical support with data collection, we thank K. Kuker, C. Birdsall, F. Perry, R. E. Fordyce, D. J. Field, T. A. Deméré, and M. deRoos. N.D.P. was supported by a National Science Foundation Graduate Research Fellowship, a postdoctoral research fellowship from the Natural Sciences and Engineering Research Council of Canada (NSERC), and by funding from the Smithsonian Institution and its Remington Kellogg Fund. J.A.G. was supported by a University Graduate Fellowship for Research from the University of British Columbia, a Scripps Postdoctoral Research Fellowship and NSERC funding to R.E.S.

## REFERENCES

**Barnes LG. 1976.** Outline of Eastern North Pacific fossil cetacean assemblages. *Systematic Zoology* **25:** 321–343.

**Bertram JEA, Biewener AA. 1992.** Allometry and curvature in the long bones of quadrupedal mammals. *Journal of Zoology* **226:** 455–467.

**Bisconti M. 2007a.** A new basal balaenopterid whale from the pliocene of northern Italy. *Palaeontology* **50:** 1103–1122.

**Bisconti M. 2007b.** Taxonomic revision and phylogenetic relationships of the rorqual-like mysticete from the Pliocene of Mount Pulgnasco, northern Italy (Mammalia, Cetacea, Mysticeti). *Palaeontographia Italica* **91:** 85–108.

**Bisconti M. 2009.** Taxonomy and evolution of the Italian Pliocene Mysticeti (Mammalia, Cetacea): a state of the art. *Bollettino Della Societa Paleontologica Italiana* **48:** 147–156.

**Bisconti M. 2010a.** A new balaenopterid whale from the late Miocene of the Stirone River, northern Italy (Mammalia, Cetacea, Mysticeti). *Journal of Vertebrate Paleontology* **30:** 943–958.

**Bisconti M. 2010b.** New description of '*Megaptera*' *hubachi* Dathe, 1983 based on the holotype skeleton held in the Museum für Naturkunde, Berlin. *Quaderni del Museo di Storia Naturale di Livorno* **23:** 37–68.

**Bisconti M, Varola A. 2000.** Functional hypothesis on an unusual mysticete dentary with double coronoid process from the Miocene of Apulia and its systematic and behavioural implications. *Palaeontographia Italica* **87:** 19–35.

**Bisconti M, Varola A. 2006.** The oldest eschrichtiid mysticete and a new morphological diagnosis of Eschrichtiidae (gray whales). *Rivista Italiana di Paleontologia e Stratigrafia* **112:** 447–457.

**Bouetel V. 2005.** Phylogenetic implications of skull structure and feeding behavior in balaenopterids (Cetacea, Mysticeti). *Journal of Mammalogy* **86:** 139–146.

**Brodie PF. 1993.** Noise generated by the jaw actions of feeding fin whales. *Canadian Journal of Zoology* **71:** 2546–2550.

**Brodie PF. 2001.** Feeding mechanics of rorquals *Balaenoptera* sp. In: Mazin JM, de Buffrenil V, eds. *Secondary adaptations of tetrapods to life in water*. Munchen: Verlag Dr. Friedrich Pfiel, 345–352.

**Clark JC, Brabb EE. 1997.** Geology of Point Reyes National Seashore and vicinity: a digital database. *U.S. Geological Survey Open-File Report* 97–456.

**Clark JC, Brabb HG, Greene HG, Ross DC. 1984.** Geology of Point Reyes Peninsula and implications for San Gregorio fault history. In: Crouch JK, Bachman SB, eds. *Tectonics and Sedimentation along the California Margin, SEPM Pacific Section*, pp. 67–85.

**Currey JD. 2002.** *Bones: structure and mechanics*. Princeton, NJ: Princeton University Press.

**Dathe F. 1983.** *Megaptera hubachi* n. sp., ein fossiler Bartenwal aus marinen Sandsteinschichten des tieferen Pliozäns Chiles. *Zeitschrift für Geologische Wissenschaften* **11:** 813–852.

**Deméré TA, Berta A, McGowen MR. 2005.** The taxonomic and evolutionary history of fossil and modern balaenopteroid mysticetes. *Journal of Mammal Evolution* **12:** 99–143.

**Deméré TA, McGowen MR, Berta A, Gatesy J. 2008.** Morphological and molecular evidence for a stepwise evolutionary transition from teeth to baleen in mysticete whales. *Systematic Biology* **57:** 15–37.

**Drake RL, Vogl AW, Mitchell AWM. 2010.** *Gray's anatomy for students*. Philadelphia, PA: Churchill Livingstone.

**Felsenstein J. 1985.** Phylogenies and the comparative method. *American Naturalist* **125:** 1–15.

**Field DJ, Campbell-Malone R, Goldbogen JA, Shadwick RE. 2010.** Quantitative computed tomography of humpback whale (*Megaptera novaeangliae*) mandibles: mechanical implications for rorqual lunge-feeding. *Anatomical Record* **293:** 1240–1247.

**Fitzgerald EMG. 2012.** Archaeocete-like jaws in a baleen whale. *Biology Letters* **8:** 94–96.

**Galloway AJ. 1977.** Geology of the Point Reyes Peninsula, Marin County, California. *California Division of Mines and Geology Bulletin* **202:** 1–72.

**Garcia GJM, da Silva JKL. 2004.** On the scaling of mammalian long bones. *Journal of Experimental Biology* **207:** 1577–1584.

**Garland T, Harvey PH, Ives AR. 1992.** Procedures for the analysis of comparative data using phylogenetically independent contrasts. *Systematic Biology* **41:** 18–32.

**Garland T, Ives AR. 2000.** Using the past to predict the present: confidence intervals for regression equations in phylogenetic comparative methods. *American Naturalist* **155:** 346–364.

**Goldbogen JA. 2010.** The ultimate mouthful: lunge feeding in rorqual whales. *American Scientist* **98:** 124–131.

**Goldbogen JA, Calambokidis J, Croll D, McKenna MF, Oleson E, Potvin J, Pyenson ND, Schorr G, Shadwick RE, Tershy B. 2012.** Scaling of lunge feeding performance in rorqual whales: mass-specific energy expenditure increases with body size and progressively limits diving capacity. *Functional Ecology* **26:** 216–226.

**Goldbogen JA, Calambokidis J, Oleson E, Potvin J, Pyenson ND, Schorr G, Shadwick RE. 2011.** Mechanics, hydrodynamics and energetics of blue whale lunge feeding: efficiency dependence on krill density. *Journal of Experimental Biology* **214:** 131–146.

**Goldbogen JA, Potvin J, Shadwick RE. 2010.** Skull and buccal cavity allometry increase mass-specific engulfment capacity in fin whales. *Proceedings of the Royal Society B* **277:** 861–868.

**Goldbogen JA, Pyenson ND, Shadwick RE. 2007.** Big gulps require high drag for fin whale lunge feeding. *Marine Ecology Progress Series* **349:** 289–301.

**Kato H, Perrin WF. 2009.** Bryde's whales *Balaenoptera edeni/brydei*. In: Perrin WF, Würsig B, Thewissen JGM, eds. *Encyclopedia of marine mammals*. Amsterdam: Academic Press, 158–163.

**Konishi K, Tamura T, Zenitani R, Bando T, Kato H, Walloe L. 2008.** Decline in energy storage in the Antarctic minke whale (*Balaenoptera bonaerensis*) in the Southern Ocean. *Polar Biology* **31:** 1509–1520.

**Lambertsen R, Ulrich N, Straley J. 1995.** Frontomandibular stay of Balaenopteridae – a mechanism for momentum recapture during feeding. *Journal of Mammalogy* **76:** 877–899.

**Lambertsen RH. 1983.** Internal mechanism of rorqual feeding. *Journal of Mammalogy* **64:** 76–88.

**Laurie AH. 1933.** Some aspects of respiration in blue and fin whales. *Discovery Reports* **7:** 363–406.

**Lillie DG. 1915.** British Antarctic 'Terra Nova' Expedition, 1910. *Natural History Report, Zoology* **1:** 85–125.

**Mackintosh NA, Wheeler JFG. 1929.** Southern blue and fin whales. *Discovery Reports* **1:** 257–540.

**Maddison WP, Maddison DR. 2011.** *Mesquite: a modular system for evolutionary analysis, Version 1.12*. Available at: http://mesquiteproject.org

**Madrid VM, Stuart RM, Verosub KL. 1986.** Magnetostratigraphy of the late Neogene Purisima Formation, Santa Cruz County, California. *Earth and Planetary Science Letters* **79:** 431–440.

**Marx FG. 2011.** The more the merrier? A large cladistic analysis of mysticetes, and comments on the transition from teeth to baleen. *Journal of Mammalian Evolution* **18:** 77–100.

**McArdle BH. 1988.** The structural relationship – regression in biology. *Canadian Journal of Zoology* **66:** 2329–2339.

**McGowen MR, Spaulding M, Gatesy J. 2009.** Divergence date estimation and a comprehensive molecular tree of extant cetaceans. *Molecular Phylogenetics and Evolution* **53:** 891–906.

**Mead JG, Fordyce RE. 2009.** The therian skull: a lexicon with emphasis on the odontocetes. *Smithsonian Contributions to Zoology* **627:** 1–216.

**Midford PE, Garland T, Maddison WP. 2005.** PDAP package of mesquite. Version 1.07.

**Orton LS, Brodie PF. 1987.** Engulfing mechanics of fin whales. *Canadian Journal of Zoology* **65:** 2898–2907.

**Parham JF, Donoghue PCJ, Bell CJ, Calway TD, Head JJ, Holroyd PA, Inoue JG, Irmis RB, Joyce WG, Ksepka DT, Patané JSL, Smith ND, Tarver JE, Van Tuinen M, Yang Z, Angielczyk KD, Greenwood J, Hipsley CA, Jacobs L, Makovicky PJ, Müller J, Smith**

**KT, Theodor JM, Warnock RCM, Benton MJ. 2012.** Best practices for justifying fossil calibrations. *Systematic Biology* **61:** 346–359.

**Pivorunas A. 1977.** Fibro-cartilage skeleton and related structures of ventral pouch of balaenopterid whales. *Journal of Morphology* **151:** 299–313.

**Pivorunas A. 1979.** Feeding mechanisms of baleen whales. *American Scientist* **67:** 432–440.

**Potvin J, Goldbogen JA, Shadwick RE. 2009.** Passive versus active engulfment: verdict from trajectory simulations of lunge-feeding fin whales *Balaenoptera physalus*. *Journal of the Royal Society Interface* **6:** 1005–1025.

**Potvin J, Goldbogen JA, Shadwick RE. 2010.** Scaling of lunge feeding in rorqual whales: an integrated model of engulfment duration. *Journal of Theoretical Biology* **267:** 437–453.

**Powell CL. 1998.** The Purisima Formation and related rocks (upper Miocene–Pliocene), greater San Francisco Bay area, central California – Review of literature and USGS collections (now housed at the Museum of Paleontology, University of California, Berkeley). *U.S. Geological Survey Open-File Report* 98–594.

**Powell CL, Barron JA, Sarna-Wojcicki AM, Clark JC, Perry FA, Brabb EE, Fleck RJ. 2007.** Age, stratigraphy, and correlations of the Late Neogene Purisima Formation, central California coast ranges. *U.S. Geological Survey Professional Papers* **1740:** 1–32.

**Pyenson ND, Goldbogen JA, Vogl AW, Szathmary G, Drake RL, Shadwick RE. 2012.** Discovery of a sensory organ that coordinates lunge feeding in rorqual whales. *Nature* **485:** 498–501.

**Pyenson ND, Sponberg SN. 2011.** Reconstructing body size in extinct crown Cetacea (Neoceti) using allometry, phylogenetic methods and tests from the fossil record. *Journal of Mammalian Evolution* **18:** 269–288.

**Rasband WS. 2012.** *Imagej*. Bethesda, MD: U. S. National Institutes of Health.

**Reeves RR, Smith TD. 2006.** A taxonomy of world whaling operation and eras. In: Estes JA, DeMaster DP, Doak TM, Williams TM, Brownell RL, Jr, eds. *Whales, whaling, and ocean ecosystems*. Berkeley, CA: University of California Press, 82–101.

**Sasaki T, Nikaido M, Hamilton H, Goto M, Kato H, Kanda N, Pastene LA, Cao Y, Fordyce RE, Hasegawa M, Okada N. 2005.** Mitochondrial phylogenetics and evolution of mysticete whales. *Systematic Biology* **54:** 77–90.

**Sasaki T, Nikaido M, Wada S, Yamada TK, Cao Y, Hasegawa M, Okada N. 2006.** *Balaenoptera omurai* is a newly discovered baleen whale that represents an ancient evolutionary lineage. *Molecular Phylogenetics and Evolution* **41:** 40–52.

**Small GL. 1971.** *The blue whale*. New York, NY: Columbia University Press, 1–248.

**Steeman ME. 2007.** Cladistic analysis and a revised classification of fossil and recent mysticetes. *Zoological Journal of the Linnean Society* **150:** 875–894.

**Steeman ME, Hebsgaard MB, Fordyce RE, Ho SYW, Rabosky DL, Nielsen R, Rahbek C, Glenner H, Sørensen MW, Willerslev E. 2009.** Radiation of extant cetaceans driven by restructuring of the oceans. *Systematic Biology* **58:** 573–585.

**True FW. 1904.** Whalebone whales of the western North Atlantic. *Smithsonian Contributions to Knowledge* **33:** 1–332.

**Vincent SE, Dang PD, Herrel A, Kley NJ. 2006.** Morphological integration and adaptation in the snake feeding system: a comparative phylogenetic study. *Journal of Evolutionary Biology* **19:** 1545–1554.

**Walsh B, Berta A. 2011.** Occipital ossification of balaenopteroid mysticetes. *Anatomical Record* **294:** 391–398.

**Werth AJ. 2000.** Feeding in marine mammals. In: Schwenk K, ed. *Feeding: form, function and evolution in tetrapod vertebrates*. New York, NY: Academic Press, 475–514.

**Westneat MW. 2004.** Evolution of levers and linkages in the feeding mechanisms of fishes. *Integrative and Comparative Biology* **44:** 378–389.

**Winston WC. 1950.** The largest whale ever weighed. *Natural History* **59:** 393–399.

**Zeigler CV, Chan GL, Barnes LG. 1997.** A new late Miocene balaenopterid whale (Cetacea: Mysticeti), *Parabalaenoptera baulinensis*, new genus and species from the Santa Cruz Mudstone, Point Reyes Peninsula, California. *Proceedings of the California Academy of Sciences* **50:** 115–133.

## SUPPORTING INFORMATION

Additional Supporting Information may be found in the online version of this article:

**Appendix S1.** Supplemental institutional abbreviations for datasets, supplemental tables, and supplemental references for morphometric and phylogenetic analyses.